High-frequency microwave signal generation using multi-transverse mode VCSELs subject to two-frequency optical injection

A. Quirce[1,2] and A. Valle[1,*]

[1]*Instituto de Física de Cantabria, CSIC-Universidad de Cantabria, Avda. Los Castros s/n, E-39005, Santander, Spain*

[2]*Departamento de Física Moderna, Universidad de Cantabria, Avda. Los Castros s/n, E-39005, Santander, Spain*

**valle@ifca.unican.es*

Abstract: In this paper we report a new method of photonic generation of microwave signals using a multi-transverse mode VCSEL subject to two-frequency optical injection. Numerical simulations show that double injection locking involving two transverse modes can be obtained in these systems. We show that the higher-order transverse mode is excited with a much larger amplitude than that of the fundamental transverse mode. The comparison with the case of a single-transverse mode VCSEL subject to similar two-frequency optical injection shows that multi-transverse mode operation of the VCSEL enhances the performance of the photonic microwave generation system. Broad tuning ranges, beyond the THz region, and narrow linewidths are demonstrated in our system. The maximum frequency of the generated microwave signals can be substantially increased if multimode VCSELs are used instead of single-mode VCSELs.

OCIS codes: (140.5960) Semiconductor lasers; (250.7260) Vertical cavity surface emitting lasers; (140.3520) Lasers, injection-locked.

References and links

1. J. Ohtsubo, *Semiconductor Lasers. Stability, Instability and Chaos*, Springer Series in Optical Sciences (Springer, 2007).
2. F. Koyama, "Recent advances of VCSEL photonics," J. Lightwave Technol. **24**(12), 4502–4513 (2006).
3. C.-H. Chang, L. Chrostowski, and C. J. Chang-Hasnain, "Injection locking of VCSELs," IEEE J. Sel. Top. Quantum Electron. **9**(5), 1386–1393 (2003).
4. D. Parekh, X. Zhao, W. Hofmann, M. C. Amann, L. A. Zenteno, and C. J. Chang-Hasnain, "Greatly enhanced modulation response of injection-locked multimode VCSELs," Opt. Express **16**(26), 21582–21586 (2008).
5. H. Li, T. Lucas, J. G. McInerney, M. Wright, and R. A. Morgan, "Injection locking dynamics of vertical cavity semiconductor lasers under conventional and phase conjugate injection," IEEE J. Quantum Electron. **32**(2), 227–235 (1996).
6. J. Altes, I. Gatare, K. Panajotov, H. Thienpont, and M. Sciamanna, "Mapping of the dynamics induced by orthogonal optical injection in vertical-cavity surface-emitting lasers," IEEE J. Quantum Electron. **42**(2), 198–207 (2006).
7. A. Valle, I. Gatare, K. Panajotov, and M. Sciamanna, "Transverse mode switching and locking in vertical-cavity surface-emitting lasers subject to orthogonal optical injection," IEEE J. Quantum Electron. **43**(4), 322–333 (2007).
8. A. Quirce, A. Valle, A. Hurtado, C. Gimenez, L. Pesquera, and M. J. Adams, "Experimental study of transverse mode selection in VCSELs induced by parallel polarized optical injection," IEEE J. Quantum Electron. **46**(4), 467–473 (2010).
9. A. Quirce, J. R. Cuesta, A. Valle, A. Hurtado, L. Pesquera, and M. J. Adams, "Polarization bistability induced by orthogonal optical injection in 1550-nm multimode VCSELs," IEEE J. Sel. Top. Quantum Electron. **18**(2), 772–778 (2012).
10. H. Lin, Y. Zhang, D. W. Pierce, A. Quirce, and A. Valle, "Polarization dynamics of a multimode vertical-cavity surface-emitting laser subject to orthogonal optical injection," J. Opt. Soc. Am. B **29**(4), 867–873 (2012).
11. C. J. Chang-Hasnain, J. P. Harbison, G. Hasnain, A. C. Vonlehmen, L. T. Florez, and N. G. Stoffel, "Dynamic, polarization, and transverse-mode characteristics of vertical cavity surface emitting lasers," IEEE J. Quantum Electron. **27**(6), 1402–1409 (1991).
12. A. Valle, J. Sarma, and K. A. Shore, "Spatial holeburning effects on the dynamics of vertical-cavity surface-emitting laser diodes," IEEE J. Quantum Electron. **31**(8), 1423–1431 (1995).

#165345 - $15.00 USD Received 23 Mar 2012; revised 13 Apr 2012; accepted 18 Apr 2012; published 30 May 2012

13. A. Hayat, A. Bacou, A. Rissons, J. C. Mollier, V. Iakovlev, A. Sirbu, and E. Kapon, "Long wavelength VCSEL-by-VCSEL optical injection locking," IEEE Trans. Microw. Theory Tech. **57**(7), 1850–1858 (2009).
14. H. Lin, D. W. Pierce, A. J. Basnet, A. Quirce, Y. Zhang, and A. Valle, "Two-frequency injection on a multimode vertical-cavity surface-emitting laser," Opt. Express **19**(23), 22437–22442 (2011).
15. S. C. Chan, R. Diaz, and J. M. Liu, "Novel photonic applications of nonlinear semiconductor laser dynamics," Opt. Quantum Electron. **40**(2-4), 83–95 (2008).
16. S. C. Chan, S. K. Hwang, and J. M. Liu, "Radio-over-fiber transmission from an optically injected semiconductor laser in period-one state," Proc. SPIE **6468,** 46811–46811 (2007).
17. S. C. Chan, "Analysis of an optically injected semiconductor laser for microwave generation," IEEE J. Quantum Electron. **46**(3), 421–428 (2010).
18. S. C. Chan, S. K. Hwang, and J. M. Liu, "Radio-over-fiber AM-to-FM upconversion using an optically injected semiconductor laser," Opt. Lett. **31**(15), 2254–2256 (2006).
19. X. Q. Qi and J. M. Liu, "Photonic microwave applications of the dynamics of semiconductor lasers," IEEE J. Sel. Top. Quantum Electron. **17**(5), 1198–1211 (2011).
20. X. Q. Qi and J. M. Liu, "Dynamics scenarios of dual-beam optically injected semiconductor lasers," IEEE J. Quantum Electron. **47**(6), 762–769 (2011).
21. Y. S. Juan and F. Y. Lin, "Photonic generation of broadly tunable microwave signals utilizing a dual-beam optically injected semiconductor laser," IEEE Photonics J. **3**(4), 644–650 (2011).
22. Y. C. Chen, Y. S. Juan, and F. Y. Lin, "High-frequency microwave signal generation in a semiconductor laser under double injection locking," Proc. SPIE **7936,** 793609 (2011).
23. A. Valle, K. A. Shore, and L. Pesquera, "Polarization selection in birefringent vertical-cavity surface emitting lasers," J. Lightwave Technol. **14**(9), 2062–2068 (1996).
24. A. Valle, J. Martin-Regalado, L. Pesquera, S. Balle, and M. San Miguel, "Polarization dynamics of birefringent index-guided vertical cavity surface-emitting lasers," Proc. SPIE **3283,** 280–291 (1998).
25. J. Y. Law, G. H. M. vanTartwijk, and G. P. Agrawal, "Effects of transverse-mode competition on the injection dynamics of vertical-cavity surface-emitting lasers," Quantum Semiclassic. Opt. J. Eu. Opt. Soc. Part B **9**(5), 737–747 (1997).
26. A. Valle and L. Pesquera, "Theoretical calculation of relative intensity noise of multimode vertical-cavity surface-emitting lasers," IEEE J. Quantum Electron. **40**(6), 597–606 (2004).
27. S. Wieczorek and W. W. Chow, "Bifurcations and chaos in a semiconductor laser with coherent or noisy optical injection," Opt. Commun. **282**(12), 2367–2379 (2009).
28. J. Martin-Regalado, F. Prati, M. San Miguel, and N. B. Abraham, "Polarization properties of vertical-cavity surface-emitting lasers," IEEE J. Quantum Electron. **33**(5), 765–783 (1997).

1. Introduction

Optical injection is a technique that is commonly employed to improve the performance of semiconductor lasers without modifying their design [1]. Attention has been paid recently on the effects of optical injection on a special type of semiconductor laser: the vertical-cavity surface-emitting laser (VCSEL) [2–10]. VCSELs have demonstrated many impressive characteristics, including low threshold current, single-longitudinal mode operation, circular beam profile and easy fabrication in large two-dimensional arrays [2]. Locking of the frequency of the injected (slave) VCSEL to the one of the injecting (master) laser has been shown for reduction of the VCSEL linewidth or for an enhancement of its modulation bandwidth [3–5]. Emission in multiple transverse modes is usually found in solitary VCSELs [11] as a result of spatial-hole burning effect [12]. The effect of single-frequency optical injection on multi-transverse mode VCSELs has been also recently studied, showing that transverse mode selection or polarization switching can appear in these systems [7–10]. Recent experimental work has also demonstrated single-mode [13] and multimode [14] VCSEL-by-VCSEL optical injection locking.

Nonlinear dynamics of optically injected semiconductor lasers can also be used for photonic microwave generation [15–22]. Compared with conventional microwave generation by electronic circuitry with multiple stages of frequency doubling, photonic microwave signal generation have the advantages of lower cost, longer transmission distance, higher speed, low power consumption, less system complexity and the ability to generate tunable microwave signals with higher frequencies [19], [21]. Photonic microwave generation find applications in radio-over-fiber (RoF) technology that holds great promise for 4G mobile communications systems [19]. Both single-beam optically injected semiconductor lasers [15–19] and dual-beam, or two-frequency, optically injected semiconductor lasers [19–22] have been considered. Tunable narrow-linewidth microwave signals have been generated by using the period-one (P1) oscillations states that appear when the semiconductor laser is subject to a

#165345 - $15.00 USD Received 23 Mar 2012; revised 13 Apr 2012; accepted 18 Apr 2012; published 30 May 2012

single-beam optical injection scheme [19]. Photonic microwaves from the P1 oscillation of an optically injected edge-emitter semiconductor laser have reached frequencies beyond 100 GHz [18]. The tuning range of the generated microwave signals is limited to several tens of GHz [21]. Recently a very high frequency (121.7 GHz) microwave signal has been generated by using a dual-beam optically injected single-mode DFB semiconductor laser [21]. Simultaneous injection of two laser beams transforms the slave laser into a dual-wavelength laser in such a way that the frequency of the generated microwave signal can be easily tuned by adjusting the frequency spacing between the two master lasers [21]. Double injection locked states are observed when the slave laser is subject to strong optical injection by both master lasers in such a way that stable locking is also observed if only light of one of the master lasers is injected [21–22]. Experimental tuning ranges, limited by the bandwidth of the photodetector, around 20 GHz were demonstrated [21]. Numerical calculations have shown that a wide continuous tuning range of more than 100 GHz is obtained by adjusting the detuning frequency of the two master lasers [22].

Characterization of the maximum microwave frequency achievable in a photonic microwave system is of interest because it sets the bandwidth limit of the system [19]. For single-beam optically injected semiconductor lasers this limit is given by the free-spectral range (around 100 GHz) because the increase of the detuning frequency necessary to achieve higher microwave frequencies causes the laser to hop to the next mode [19]. The highest frequency that can be generated in a dual-beam optically injected semiconductor laser is limited by the locking range determined by the maximum injection strengths of the two master lasers [21].

In this work we propose a new method of photonic generation of microwave signals using a multi-transverse mode VCSEL subject to two-frequency optical injection. The dynamics of the two transverse modes of a VCSEL is found using the model of [7] extended to consider dual-beam optical injection. In contrast to the experimental results of [14] in which optical injection is orthogonally polarized to the linear polarization of the transverse modes, we now consider the same linear polarization for both optical injections and transverse modes. Our calculations show that double injection locking involving the two transverse modes can be obtained in these systems. We show that the higher-order transverse mode is excited with a much larger amplitude than that of the fundamental transverse mode. The comparison with the case of a similar single-transverse mode VCSEL subject to the same two-frequency optical injection shows that the extra degree of freedom given by the multi-transverse mode operation of the VCSEL is useful for enhancing the performance of the photonic microwave generation system. In fact we obtain that the amplitude of the total power generated by multi-transverse mode VCSELs is much larger than that obtained with a similar single-transverse mode VCSEL subject to the same two-frequency optical injection. This shows that while for single-frequency injection, excitation of a second mode is detrimental for photonic generation of microwave signals [19], for two-frequency injection, excitation of a second mode is beneficial. Wide tuning ranges and narrow linewidths are also demonstrated in our system.

2. Theoretical model

The theoretical model is based on a spatially dependent dynamical model of a multi-transverse mode VCSEL subject to single-frequency optical injection [7]. In this paper we extend it for considering a two-frequency optical injection. The simulated cylindrically symmetric weak index-guided structure, together with the complete details of the model can be found in [7]. The model describes the complex amplitudes of two transverse modes with their two possible linear polarizations. Subscripts x and y will be used to denote the two orthogonal linear polarization directions. The appropriate transverse modes of the structure are the LP_{mn} modes. Here we treat the case of VCSELs that can operate in the fundamental (LP_{01}) and in the first order (LP_{11}) transverse modes. Subscripts 0,1 will be used to denote the LP_{01} and LP_{11} modes, respectively. The equations describing the polarization and transverse mode behavior of the VCSEL with a two-frequency injected optical field read as [7]

#165345 - $15.00 USD Received 23 Mar 2012; revised 13 Apr 2012; accepted 18 Apr 2012; published 30 May 2012

$$\dot{E}_{0x} = k(1+i\alpha)\left(E_{0x}(g_{0x}-1)+iE_{0y}g_{0xy}\right)-(\gamma_a+i\gamma_{p0})E_{0x}+\frac{\kappa_{01}}{\tau_{\text{in}}}e^{i\Delta\omega_1 t}+\frac{\kappa_{02}}{\tau_{\text{in}}}e^{i\Delta\omega_2 t} + \sqrt{\frac{\beta}{2}}\left(\sqrt{\bar{N}+\bar{n}}\,\xi_{0+}+\sqrt{\bar{N}-\bar{n}}\,\xi_{0-}\right) \tag{1}$$

$$\dot{E}_{0y} = k(1+i\alpha)\left(E_{0y}(g_{0y}-1)-iE_{0x}g_{0yx}\right)+(\gamma_a+i\gamma_{p0})E_{0y}-i\ 0\left(\sqrt{\bar{N}+\bar{n}}\,\xi_{0+}-\sqrt{\bar{N}-\bar{n}}\,\xi_{0-}\right) \tag{2}$$

$$\dot{E}_{1x} = k(1+i\alpha)\left(E_{1x}(g_{1x}-\kappa_r)+iE_{1y}g_{1xy}\right)+i\gamma_p^{tr}E_{1x}-(\gamma_a+i\gamma_{p1})E_{1x}+\frac{\kappa_{11}}{\tau_{\text{in}}}e^{i\Delta\omega_1 t}+\frac{\kappa_{12}}{\tau_{\text{in}}}e^{i\Delta\omega_2 t} + \sqrt{\frac{\beta}{2}}\left(\sqrt{\bar{N}+\bar{n}}\,\xi_{1+}+\sqrt{\bar{N}-\bar{n}}\,\xi_{1-}\right) \tag{3}$$

$$\dot{E}_{1y} = k(1+i\alpha)\left(E_{1y}(g_{1y}-\kappa_r)-iE_{1x}g_{1yx}\right)+i\gamma_p^{tr}E_{1y}+(\gamma_a+i\gamma_{p1})E_{1y} -i\sqrt{\frac{\beta}{2}}\left(\sqrt{\bar{N}+\bar{n}}\,\xi_{1+}-\sqrt{\bar{N}-\bar{n}}\,\xi_{1-}\right) \tag{4}$$

$$\frac{\partial N(r,t)}{\partial t} = I(r)+D\nabla_{\perp}^2 N-\gamma_e\left[N\left(1+\sum_{i=0,1}\sum_{j=x,y}\left|E_{ij}\right|^2\psi_{ij}^2(r)\right)-in\sum_{i=0,1}(E_{ix}E_{iy}^*-E_{iy}E_{ix}^*)\psi_{ix}(r)\psi_{iy}(r)\right] \tag{5}$$

$$\frac{\partial n(r,t)}{\partial t} = -\gamma_s n+D\nabla_{\perp}^2 n-\gamma_e\left[n\sum_{i=0,1}\sum_{j=x,y}\left|E_{ij}\right|^2\psi_{ij}^2(r)-iN\sum_{i=0,1}(E_{ix}E_{iy}^*-E_{iy}E_{ix}^*)\psi_{ix}(r)\psi_{iy}(r)\right] \tag{6}$$

where E_{0j} and E_{1j} are the complex amplitudes of the LP_{01} and LP_{11} modes (the subindex j stands for the linear polarization state of the given mode), $N(r,t)$ is the total carrier number, $n(r,t)$ is the difference in the carrier numbers of the two magnetic sublevels, and ψ_{0j} and ψ_{1j} are the modal intensity profiles of the LP_{01} and LP_{11} modes obtained by solving the Helmholtz Eq [23–24], respectively. κ_r is the relative loss of the LP_{11} mode with respect to the LP_{01} mode. It determines the value of the injection current at which the LP_{11} mode begins lasing. $I(r)$ represents a uniform current injection over a circular disc of 6 μm radius, and then $I(r) = I$ if $r<6\ \mu m$, and $I(r) = 0$, elsewhere. The normal gain normalized to the threshold gain, g_{ij} $(i = 0,1, j = x, y)$, and g_{ijk} $(i = 0,1; jk = xy,yx)$ are given by

$$g_{i,jk} = \frac{\int_0^{\infty} n(r,t)\psi_{ij}(r)\psi_{ik}(r)rdr}{\int_0^{\infty}\psi_{ij}^2(r)rdr} \qquad g_{ij} = \frac{\int_0^{\infty} N(r,t)\psi_{ij}^2(r)rdr}{\int_0^{\infty}\psi_{ij}^2(r)rdr} \tag{7}$$

In the two-frequency injection scheme the VCSEL is optically injected by a master laser 1 (ML1) and a master laser 2 (ML2), with optical frequencies ω_1 and ω_2, respectively. Two frequency detunings, $\Delta\omega_1 = \omega_1-\omega_{th}$ and $\Delta\omega_2 = \omega_2-\omega_{th}$, with respect to the central frequency between the two polarizations of the fundamental mode $\omega_{th} = (\omega_{0x} + \omega_{0y})/2$, appear in the Eqs. The injection terms only appear in the Eqs. for E_{0x} and E_{1x}, hence linearly polarized optical injection in the x-direction is considered for both master lasers. In this way if the solitary VCSEL emits only in the x-linear polarization, as it will be considered in this work, the directions of the polarizations of optical injections and VCSEL are parallel. Optical injection terms are also characterized by the injection strengths, k_{im}, and the VCSEL roundtrip

#165345 - $15.00 USD Received 23 Mar 2012; revised 13 Apr 2012; accepted 18 Apr 2012; published 30 May 2012

time, $\tau_{in} = 2L/v_g$, where v_g is the group velocity. The injection strength k_{im} ($i = 0,1$, $m = 1,2$) is given by

$$k_{im} = \left(\frac{1}{\sqrt{R}} - \sqrt{R} \right) \sqrt{\eta_{inj}} \sqrt{P_{inj,im}} \tag{8}$$

where R is the output-mirror reflectivity, η_{inj} is the coupling efficiency of the injected light to the optical field in the laser cavity and $P_{inj,im}$ is the power injected in the i-transverse mode by the m-master laser [25]. In this work we choose the k_{im} values in relation to what should be expected when light from a multi-transverse mode VCSEL is injected into a similar device. k_{01} (k_{12}) is related to the spatial overlap integral between the profiles of the fundamental modes (the higher-order modes) of master and slave lasers. Then a reasonable choice is $k_{01} = k_{12} = k_s$, where k_s is the injection strength between similar transverse modes. k_{02} (k_{11}) is related to the spatial overlap integral between the profiles of the fundamental mode of the slave and the higher order mode of the master (higher-order mode of the slave and the fundamental mode of the master) VCSEL. In this way we choose $k_{02} = k_{11} = k_c$, with $k_c \leq k_s$, where k_c is a "crossed" injection strength between transverse modes with different order. The frequency splitting between the orthogonal polarizations of the LP_{01} mode, $2\gamma_{p0}/(2\pi)$, between the orthogonal polarizations of the LP_{11} mode, $2\gamma_{p1}/(2\pi)$, and between the two transverse modes with the same polarization, $\gamma_p^{tr}/(2\pi)$, are obtained from the calculation of the waveguide modes via the Helmholtz equation [23–24]. We have chosen the values of refractive indexes $n_{core,x}$, $n_{core,y}$ and n_{cladd} in such a way that $2\gamma_{p0}/(2\pi)$ = 10 GHz and $\gamma_p^{tr}/(2\pi)$ = 63 GHz. Spontaneous emission noise processes are modeled by the terms $\xi_{\pm}$ taken as complex Gaussian white noise sources of zero mean and delta-correlated in time. In the noise terms we consider integrated over the active region carrier distributions, $\bar{N}$ and $\bar{n}$ [7]. The rest of the parameters that appear in the Eqs. and their meaning are specified in the Table 1. Time and space integration steps of 0.01 ps and 0.12 microns, respectively, have been used. The boundary conditions for the carrier distribution are taken as $N(\infty,t) = 0$, $n(\infty,t) = 0$. The initial conditions correspond to a below threshold stationary solution, i.e to $I = 0.1I_{th}$, where I_{th} is the threshold current.

Table 1. Parameters Used in the Model

SYMBOL	VALUE	MEANING OF THE SYMBOL
a	6 μm	Radius of the core region
L	1 μm	Length of the cavity
$n_{core,x}$	3.5001025	Refractive index of the core region in the x-direction
$n_{core,y}$	3.5	Refractive index of the core region in the y-direction
n_{cladd}	3.41	Refractive index of the cladding region
K	300 ns^{-1}	Field decay rate
α	3	Linewidth enhacement factor
γ_e	0.55 ns^{-1}	Decay rate for the total carrier population
γ_s	1000 ns^{-1}	Spin-flip relaxation rate
D	10 cm^2s^{-1}	Diffusion coefficient
β	10^{-5} ns^{-1}	Spontaneous emission coefficient
γ_a	–0.3 ns^{-1}	Dichroism
η_{inj}	1	Coupling efficiency
R	0.995	Output-mirror reflectivity

3. Two-frequency optically injected single-mode VCSELs

In this section, we present the results corresponding to the two-frequency optical injection on a VCSEL emitting only in the fundamental transverse mode. We have chosen a value $\kappa_r = 10$ to assure $LP_{01,x}$ mode operation. Results are given in terms of the separation between the frequencies of the two master lasers, $\Delta f = (\omega_2-\omega_1)/(2\pi)$, the frequency detuning of ML1 with respect to the frequency of the $LP_{01,x}$ mode, $\Delta\nu$, and the injection strength κ_s. We show in Fig. 1(a) the dynamical evolution of a free-running single-transverse mode VCSEL when switched-on at time $t>0$ with a $I = 1.8I_{th}$ bias current value. The VCSEL emits in the steady

#165345 - $15.00 USD Received 23 Mar 2012; revised 13 Apr 2012; accepted 18 Apr 2012; published 30 May 2012

state in the $LP_{01,x}$ mode with a single peaked RF spectrum appearing at the relaxation oscillation frequency. Spectra are calculated after a transient time of 14 ns.

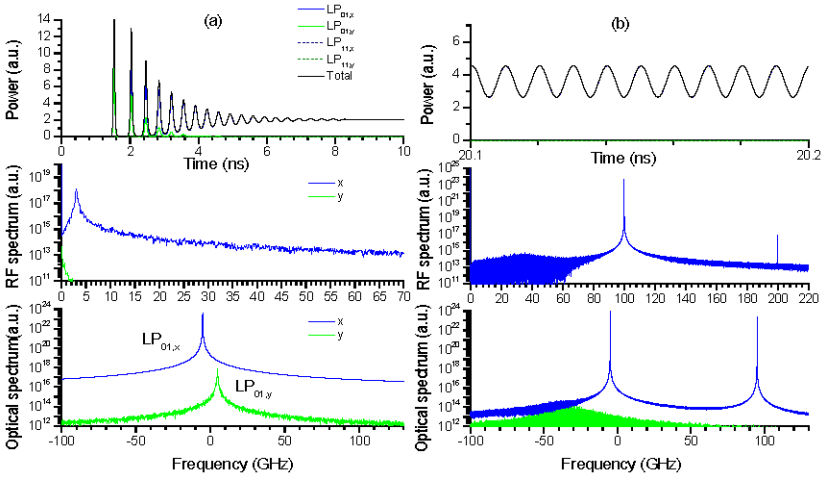

Fig. 1. Temporal and spectral dynamics of a single-transverse mode VCSEL when (a) no optical injection is applied, (b) $\Delta f = 100$ GHz, $\Delta\nu = 0$ GHz, $\kappa_s = 10^{-2}$, and $\kappa_c = \kappa_s/2$. Upper row: Time traces of the power of the polarized transverse modes. Middle row: RF spectra of the polarized powers. Lower row: *x* and *y*-polarized optical spectra.

Figure 1(b) shows the results for an injection strength of $\kappa_s = 10^{-2}$, $\Delta f = 100$ GHz, and with the frequency of ML1 just at the $LP_{01,x}$ mode frequency. An almost sinusoidal time trace is obtained for the power of $LP_{01,x}$ mode, that is the only mode with nonnegligible power. The frequency of this sinusoidal modulation is Δf. The optical spectrum consists of two well defined peaks at the ML1 and ML2 optical frequencies and the RF spectrum has a very narrow peak at Δf, the frequency separation between ML2 and ML1. This situation is similar to the double injection locking that has been obtained using a single mode DFB laser subject to dual-beam injection [21] and in simulations using a single-mode rate equation model [22].

4. Two-frequency optically injected multi-transverse mode VCSELs

We now present the results corresponding to two-frequency optical injection on a multi-transverse mode VCSEL. This laser is exactly the same than the single-transverse mode VCSEL but changing the parameter κ_r to a smaller value ($\kappa_r = 1.022$) for which both transverse modes have rather similar losses. Results obtained for the solitary multimode VCSEL ($\kappa_s = \kappa_c = 0$) are plotted in Fig. 2(a). In this case the VCSEL shows a steady-state in which both transverse modes, LP_{01} and LP_{11}, are excited in the *x*-direction. The steady-state total power in Fig. 2(a) is 1.7, a similar value to the value, 2.1, that was obtained for Fig. 1(a). The power in the $LP_{11,x}$ mode is only slightly larger than that of $LP_{01,x}$. Fig. 2(a) shows that the *x*-polarized RF spectrum has two peaks that appear due to the multi-transverse mode character of the VCSEL [26]. The multimode character of the system is also clear from the optical spectra of Fig. 2(a). The separation between $LP_{01,x}$ and $LP_{11,x}$, similar to the separation between $LP_{01,y}$ and $LP_{11,y}$, is around 63 GHz.

Figure 2(b) shows the results of the multi-transverse mode VCSEL subject to two-frequency optical injection. The levels of the injection strengths, Δf, and $\Delta\nu$ are equal to those considered in the single-transverse mode case (Fig. 1(b)). In this way we can compare the performance of microwave generating systems using single and multi-transverse mode VCSELs. Similarly to Fig. 1(b), Fig. 2(b) also shows the double injection locking phenomenon. Again, two well defined peaks at the frequencies of ML1 and ML2 are observed in the *x*-polarized optical spectrum resulting in a RF spectrum with a narrow peak at the Δf frequency. But Fig. 2(b) also shows an interesting and novel feature when compared to Fig. 1(b): the high-order transverse mode $LP_{11,x}$ is excited with a much larger amplitude than that

#165345 - $15.00 USD Received 23 Mar 2012; revised 13 Apr 2012; accepted 18 Apr 2012; published 30 May 2012

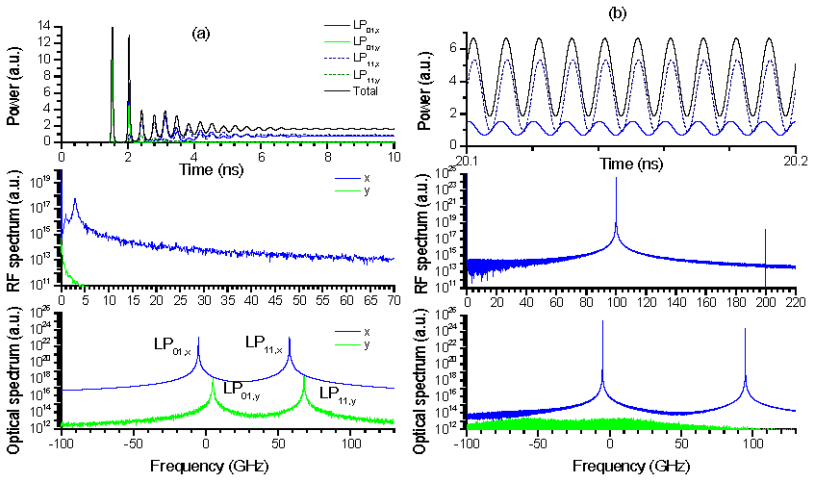

Fig. 2. Temporal and spectral dynamics of a multi-transverse mode VCSEL when (a) no optical injection is applied, (b) Δf = 100 GHz, $\Delta\nu$ = 0 GHz, $\kappa_s = 10^{-2}$, and $\kappa_c = \kappa_s/2$. Upper row: Time traces of the power of the polarized transverse modes. Middle row: RF spectra of the polarized powers. Lower row: *x* and *y*-polarized optical spectra.

of the $LP_{01,x}$ mode. The power of both transverse modes oscillate with a phase difference near $\pi/2$. In this way the variation of the total power is nearly sinusoidal, as shown in the time traces and RF spectrum of Fig. 2(b). Interestingly, the amplitude of the total power is much larger than the one obtained with the equivalent single-transverse mode VCSEL case illustrated in Fig. 1(b). This shows that the amplitude of the microwave signal generated by two-frequency optical injection is enhanced if multi-transverse mode operation in the VCSEL is considered instead single-transverse mode operation.

5. Comparison between single and multi-transverse mode cases

In this section we make a detailed comparison between the two-frequency optical injection in single and multi-transverse mode VCSELs. Figure 3(a) shows the results of the multi-transverse mode VCSEL subject to two-frequency optical injection when increasing Δf and with similar conditions to those of Fig. 2(b). Sinusoidal time traces are obtained for the power of $LP_{01,x}$, $LP_{11,x}$ modes and total power. The amplitude of the oscillations decreases as Δf increases. We have also included the time trace corresponding to the single-transverse mode VCSEL to show that the enhancement due to multi-mode operation is maintained. We show in Fig. 4(a) the peak-to-peak amplitude of the total power as a function of Δf. Results for single and multi-transverse mode VCSELs, A_{sm} and A_{mm} respectively, are included. Also results for two injection strength levels are shown. All the cases reported in this fig. have an almost sinusoidal variation of the total power. Peak-to-peak amplitudes decrease as Δf increases. An increase of the injection strength κ_s leads to larger peak-to-peak amplitudes for both, single and multi-transverse mode cases. This is also illustrated in Fig. 3(b) in which κ_s is increased with respect to Fig. 3(a). For all the values of Δf and κ_s the amplitude of the oscillation obtained with multi-transverse mode VCSELs is larger than that obtained for single-transverse mode VCSELs as it is shown in Fig. 4(a). This enhancement is quantified in Fig. 4(b), in which the ratio between peak-to-peak amplitudes of the total power obtained for multi and single-mode devices, A_{mm}/A_{sm}, is plotted as a function of Δf. A maximum value of 2.6 is obtained for $\kappa_s = 10^{-2}$ at Δf = 63.4 GHz, value that is very near the transverse mode separation. A not so well defined maximum is obtained for $\kappa_s = 3\ 10^{-2}$ at Δf = 100 GHz. These values are near the 63 GHz transverse mode separation indicating that maximum enhancement is obtained when the optical frequencies of ML1 and ML2 are close to the frequencies of the free-running $LP_{01,x}$, and $LP_{11,x}$ modes, respectively.

#165345 - $15.00 USD Received 23 Mar 2012; revised 13 Apr 2012; accepted 18 Apr 2012; published 30 May 2012

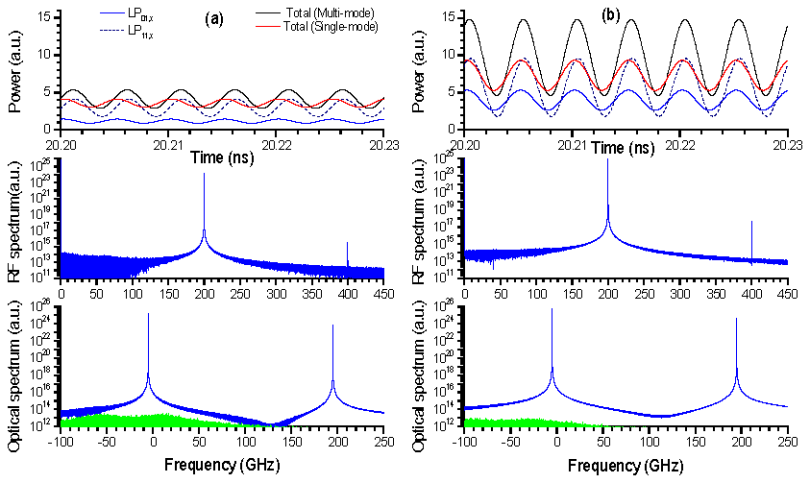

Fig. 3. Temporal and spectral dynamics of a multi-transverse mode VCSEL when (a) Δf = 200 GHz, $\kappa_s = 10^{-2}$ (b) Δf = 200 GHz, $\kappa_s = 3\ 10^{-2}$. Other parameters are $\Delta\nu = 0$ GHz and $\kappa_c = \kappa_s/2$. Upper row: Time traces of the power of the polarized transverse modes and total power. Total power for the single-mode case is also included. Middle row: RF spectra of the polarized powers. Lower row: *x* and *y*-polarized optical spectra.

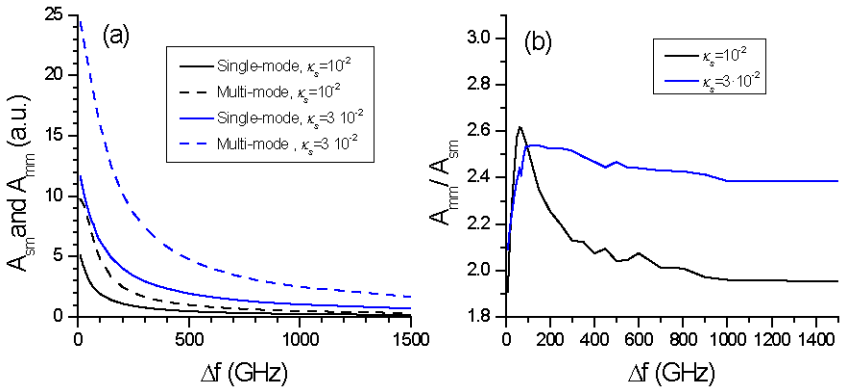

Fig. 4. (a) Peak-to-peak amplitude of the total power as a function of Δf. (b) Ratio between peak-to-peak amplitudes obtained with multi-transverse and single transverse-mode VCSELs. In this Fig. $\Delta\nu = 0$ and $\kappa_c = \kappa_s/2$.

Figure 4(a) also shows that the largest variations of peak-to-peak amplitudes with Δf occur in the microwave region (<300 GHz). In Fig. 4 we have also considered a Δf range that goes beyond the microwave range. In this region the generated radiation has appreciable amplitude that increases as κ_s is increased. The amplitude of this modulation slightly decreases when Δf is in the THz region. An example of the dynamical evolution obtained for Δf = 500 GHz, a value larger than those of the microwave region, is shown in Fig. 5(a). Single and multimode VCSELs are able to respond at 500 GHz with appreciable amplitudes. The response of multimode VCSELs is such that the power of both transverse modes oscillates nearly in phase.

Figure 6(a) shows the dependence of A_{mm} and A_{sm} on the injection strength κ_s. Results are also given in terms of the injection ratio defined as the ratio of the injected optical power by the *m*-master laser, ($P_{inj,0m} + P_{inj,1m}$) versus the output power of the free-running multimode VCSEL. Both A_{mm} and A_{sm} increase with κ_s . Double injection locking is observed when κ_s is larger than 2.5 10^{-3} and 2.9 10^{-3} for single and multimode VCSELs, respectively.

#165345 - $15.00 USD Received 23 Mar 2012; revised 13 Apr 2012; accepted 18 Apr 2012; published 30 May 2012

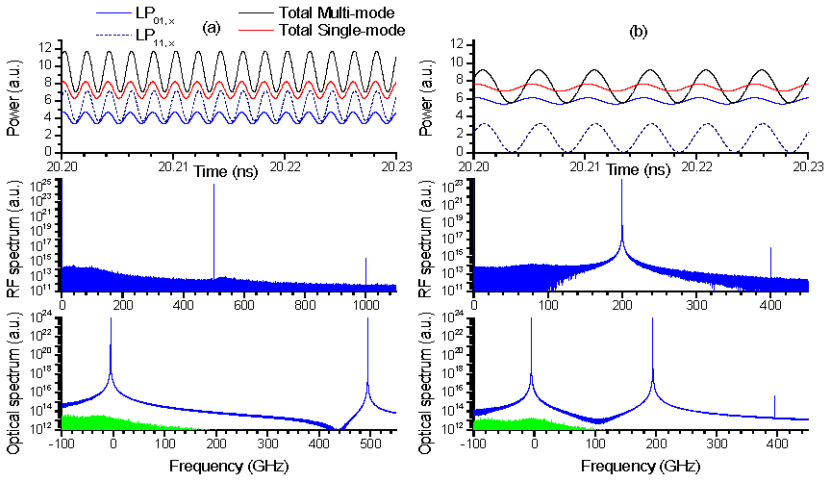

Fig. 5. Temporal and spectral dynamics of a multi-transverse mode VCSEL when (a) Δf = 500 GHz, κ_s = 3 10^{-2}, $\kappa_c = \kappa_s/2$, $\Delta\nu$ = 0 GHz (b) Δf = 200 GHz, κ_s = 3 10^{-2}, $\kappa_c = 0.1\kappa_s$, $\Delta\nu$ = 0 GHz. Upper row: Time traces of the power of the polarized transverse modes. Middle row: RF spectra of the polarized powers. Lower row: *x* and *y*-polarized optical spectra.

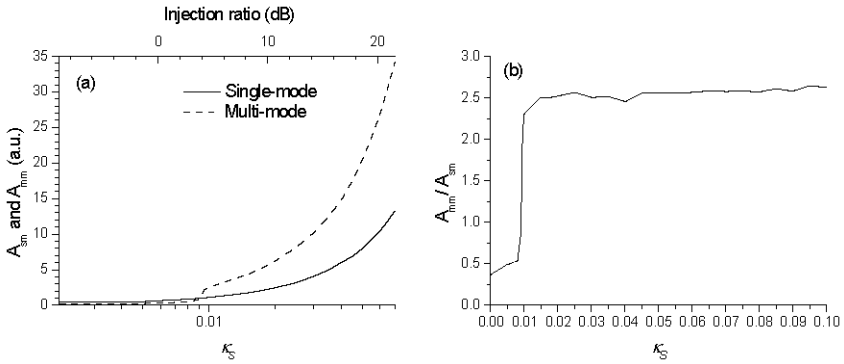

Fig. 6. (a) Peak-to-peak amplitude of the total power as a function of κ_s. (b) Ratio between peak-to-peak amplitudes obtained with multi and single transverse-mode VCSELs. In this Fig. $\kappa_c = \kappa_s/2$, Δf = 200 GHz, and $\Delta\nu$ = 0 GHz.

The curve for multi-transverse mode VCSELs has a small step near $\kappa_s = 10^{-2}$ that is due to a sudden change of the phase difference between the power time series of both transverse modes: that phase difference is near π if $\kappa_s \leq 9\ 10^{-3}$ and changes to a value near $\pi/2$ at $\kappa_s = 10^{-2}$. Above the κ_s value for which the step in A_{mm} is observed, the ratio A_{mm}/A_{sm}, has an almost constant value of 2.6, as it is shown in Fig. 6(b).

Figure 7(a) shows the dependence of A_{mm} and A_{sm} on the injection strength κ_c for two different values of κ_s. Both A_{mm} and A_{sm} increase with κ_c. Note that all amplitudes vanish when $\kappa_c \to 0$. For the single-mode VCSEL with double injection this means that the VCSEL recovers the locked state with single-frequency optical injection characterized by a constant value of the power. For the two-mode VCSEL the situation can be explained as follows. If only injection from ML1 (ML2) with no coupling to the $LP_{11,x}$ ($LP_{01,x}$) mode is considered, for instance κ_{01} = 3 10^{-2}, $\kappa_{12} = \kappa_c = 0$ (κ_{12} = 3 10^{-2}, $\kappa_{01} = \kappa_c = 0$) the optical spectrum of the VCSEL consists on a single peak at the ML1 (ML2) frequency, the power of $LP_{01,x}$ ($LP_{11,x}$) is constant and the RF spectrum is flat. If injection from ML1 and ML2 is considered such that $\kappa_{01} = \kappa_{12}$ = 3 10^{-2}, $\kappa_c = 0$, the optical spectrum of the VCSEL consists on two peaks at the ML1 and ML2 frequencies, the powers of both modes, $LP_{01,x}$ and $LP_{11,x}$, are constant and the

#165345 - $15.00 USD Received 23 Mar 2012; revised 13 Apr 2012; accepted 18 Apr 2012; published 30 May 2012

RF spectrum keeps on being flat. A nonzero value of κ_c is enough for the RF spectrum to develop a peak and for both modes to oscillate at the Δf frequency. This shows that the reason for the transverse modes power oscillations is the nonzero value of the κ_c injection strength.

Figure 7(a) shows that for large values of κ_s, $A_{mm} > A_{sm}$. However, for $\kappa_s = 10^{-2}$, $A_{mm} \leq A_{sm}$ until the curve for multi-transverse mode VCSELs has a small step near $\kappa_c / \kappa_s = 0.42$. This step is again due to a sudden change of the phase difference between the power time series of both transverse modes: that phase difference is near π if $\kappa_c/\kappa_s \leq 0.4$ and changes to a value near $\pi/2$ at $\kappa_c/\kappa_s = 0.45$. Figure 7(b) shows the ratio A_{mm}/A_{sm} corresponding to data of Fig. 7(a). Larger enhancement of A_{mm} with respect to A_{sm} can be obtained when κ_c is small providing that κ_s is large enough. This situation is illustrated in Fig. 5(b) for which a value of $A_{mm}/A_{sm} = 4.3$ is reached.

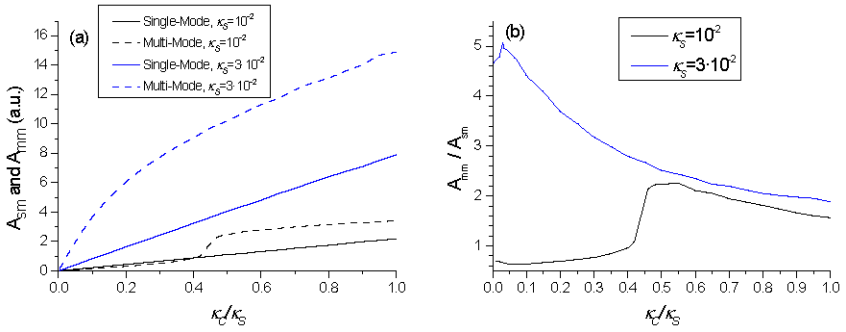

Fig. 7. (a) Peak-to-peak amplitude of the total power as a function of κ_c / κ_s. (b) Ratio between peak-to-peak amplitudes obtained with multi and single transverse-mode VCSELs. In this Fig. Δf = 200 GHz, and $\Delta \nu$ = 0 GHz.

The dependence of A_{mm} and A_{sm} on the bias current of the VCSEL is analyzed in Fig. 8(a). Both quantities increase with the bias current. However the ratio A_{mm}/A_{sm} slightly decrease in a linear way with I. For instance, when $\kappa_s = 3\ 10^{-2}$, it goes from 2.6 at $I/I_{th} = 1.2$ to 2.2 at $I/I_{th} = 8$. We have also analyzed the effect of the frequency detuning, $\Delta\nu$, on the dynamics of the system. Dynamics obtained for the multimode case when $\Delta\nu = 5$ GHz and $\Delta\nu = -5$ GHz are very similar to those obtained when $\Delta\nu = 0$ GHz, providing that the system is in the double injection locked regime. This indicates that there is an appreciable range of $\Delta\nu$ for which the enhancement of the amplitude of the generated microwave signal due to high-order transverse mode excitation does not depend on the $\Delta\nu$ value. The relative phase between the power time series corresponding to the $LP_{01,x}$ and $LP_{11,x}$ modes in the double-injection locked multi-transverse mode VCSEL can change depending on the injection conditions. Comparison between Fig. 3(a) and Fig. 3(b) indicates that it decreases as the value of the κ_s injection strength increases.

We have also calculated the RF linewidths of the signals generated by double-injection locking of multi-transverse mode VCSELs. In this paper most spectra have been calculated with a temporal window of 1.05 μs and with a maximum frequency of 2000 GHz. Then linewidths are measured with a 0.95 MHz frequency resolution. We have considered in our calculations a finite linewidth of the optical spectrum of both master lasers. This effect has been included by considering phase fluctuations in the two external signals as in Ref [27]. Equal linewidths and independent phase fluctuations have been considered for both master lasers. 3-dB RF linewidths are shown in Fig. 8(b) as a function of the linewidth of the optical spectrum of one of the MLs. Narrow linewidths, in the MHz range, are demonstrated like in [21–22]. RF linewidth increases with the injection linewidth. The RF linewidth is almost twice the injection linewidth of the ML if this ≥ 1 MHz. In all the RF spectra the obtained sidemode suppression ratio has been more than 50 dB, like in [21]. The second largest peak is the first harmonic corresponding to the peak that appears at Δf.

#165345 - $15.00 USD Received 23 Mar 2012; revised 13 Apr 2012; accepted 18 Apr 2012; published 30 May 2012

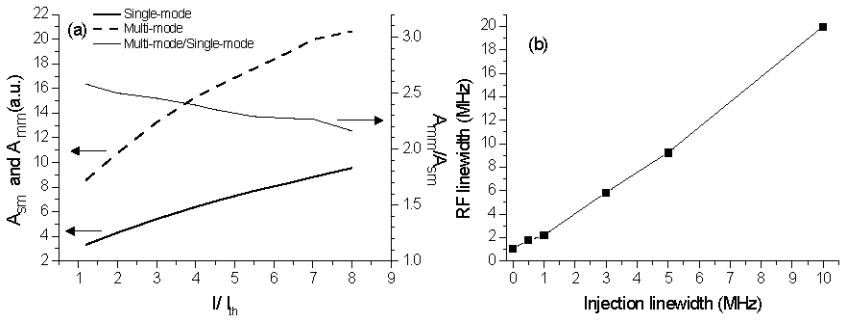

Fig. 8. (a) Peak-to-peak amplitude of the total power as a function of I/I_{th} when Δf = 200 GHz and κ_s = 3 10^{-2} (b) RF linewidth as a function of the linewidth of the master lasers when Δf = 100 GHz and κ_s = 10^{-2}. In this Fig. $\kappa_c = \kappa_s/2$ and $\Delta\nu$ = 0 GHz.

6. Discussion and conclusions

Peak-to-peak amplitudes in this work have been given in the arbitrary units used in the spin-flip model [28]. An idea of the magnitude of the power corresponding to the peak-to-peak amplitudes obtained in this work can be obtained by taking typical values of the power emitted by a VCSEL with 12 μm diameter like the one simulated in this paper. For instance, for a typical value of the total power~0.4 mW for I/I_{th} = 1.8, A_{mm} (mW) = 0.235A_{mm} (a.u.). For the conditions of Fig. 2(b) this corresponds to a 1.1 mW peak-to-peak amplitude for 1.17 mW of power injected by each ML.

The model that we have used includes the polarization degree of freedom of transverse modes. In our case the role played by *y*-polarized transverse modes has been negligible because we have considered an optical injection that is parallel to the *x*-polarization of the solitary VCSEL. Preliminary work using an extension of this model to consider orthogonally polarized optical injection indicates that the results obtained in this work are maintained. This result is of interest to show that the proposed microwave signal generation system is independent on the polarization of the master lasers. In our calculations we have assumed that the κ_c parameter that represents the "crossed" injection strength between transverse modes of different order is equal for LP_{01} injected into LP_{11} and for LP_{11} injected into LP_{01} mode. Since this is a simplification in our model, future work is intended to know if the results obtained in this work are maintained when asymmetric "crossed" injection strengths are considered. Also in our calculations we have considered a high value of the γ_s parameter such that the results of the simulations should be the same if the carrier difference *n* is set equal to 0 (i.e., if integration of the equations with only the total carrier density is performed). Future work is also planned to investigate the influence of smaller values of the γ_s parameter, and hence of the spin of the carriers on our results.

Figure 4 shows that a typical increase in the amplitude obtained with multimode VCSELs with respect to single-mode VCSELs is between 2 and 3. We discuss now the corresponding increase in the maximum frequency of the generated microwave signals. Assuming that amplitudes larger than a value A are required, we calculate the maximum value of the microwave frequency obtained with the single-mode VCSEL, $\Delta f_{max,sm}$, such that A_{sm} >A if Δf <$\Delta f_{max,sm}$. We also calculate the corresponding quantity for the multimode VCSEL, $\Delta f_{max,mm}$, given by A_{mm} >A if Δf <$\Delta f_{max,mm}$. Figure 9 shows the results for A = 4 a.u. as a function of the injection strength or the injection ratio. The maximum frequency increases significantly when using multimode VCSELs instead of single-mode VCSELs. For instance the maximum frequency increases from 193 GHz to 578 GHz for an injection ratio of 14 dB.

Summarizing, in this work we have made a theoretical study of the dynamical properties of single and multi-transverse mode VCSELs when they are subject to two-frequency optical injection. We have focused our analysis in the double injection locking observed at large injection strengths, useful for photonic microwave signal generation. Numerical simulations

#165345 - $15.00 USD Received 23 Mar 2012; revised 13 Apr 2012; accepted 18 Apr 2012; published 30 May 2012

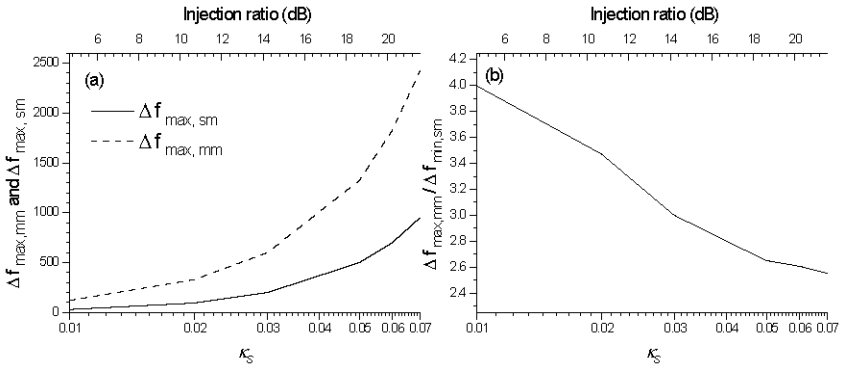

Fig. 9. (a) Maximum frequency of the generated microwave signals as a function of the injection strength. (b) Ratio of the maximum frequencies obtained with multimode and single-mode VCSELs. In this Fig. A = 4 a.u., $\kappa_c = \kappa_s/2$ and $\Delta\nu = 0$ GHz.

of single and multi-transverse mode VCSELs have shown that the double injection locking can be obtained when these devices are subject to two-frequency optical injection. For the case of multimode VCSELs we have shown that the response of multi-transverse mode VCSELs under two-frequency optical injection is larger than that obtained with similar single-transverse mode VCSELs. In this way high-order transverse mode excitation enhances the performance of the photonic microwave generation system based on two-frequency optical injection. This shows that while for single-frequency injection, excitation of a second mode is detrimental for generating microwave signals [19], for two-frequency injection, excitation of a second mode is beneficial. Narrow linewidths are demonstrated in our system. Broad tuning ranges, beyond the THz region, have been determined in terms of the characteristics of the optical injection and of the transverse mode properties of the VCSEL. The maximum frequency of the generated microwave signals can be substantially increased if multimode VCSELs are used instead of single-mode VCSELs.

Acknowledgments

The authors acknowledge support from the Ministerio de Ciencia e Innovación under project TEC2009-14581-C02-02. A. Q. was supported in part by the Fondo Social Europeo (FSE) under the programme Junta de Ampliación de Estudios (JAE-predoc).

#165345 - $15.00 USD Received 23 Mar 2012; revised 13 Apr 2012; accepted 18 Apr 2012; published 30 May 2012